*Inorg. Chem.* **2002**, *41*, 7024–7030


# Polytypism in Columnar Group 14 Halide Salts: Structures of $(Et_2NH_2)_3Pb_3X_9 \cdot nH_2O$ (X = Cl, Br) and ($\beta$-alaninium)$_2SnI_4$

**Roger D. Willett* and Karen R. Maxcy**

*Department of Chemistry, Washington State University, Pullman, Washington 99164*

**Brendan Twamley**

*University Research Office, University of Idaho, Moscow, Idaho 83843*

Received July 15, 2002

The crystal structures of three hybrid organoammonium metal halide salts composed of edge-sharing $MX_6$ octahedra have been determined. The genesis of these structures can be traced to the parent hexagonal $MX_2$ structure via dimensional reduction and recombination arguments. The structures of $(Et_2NH_2)_3Pb_3X_9 \cdot nH_2O$ (X = Br, I) contain unique columnar $(Pb_3X_9)_n^{3n-}$ structures, built up of edge-shared $PbX_6$ octahedra. The interaction of the $Et_2NH_2^+$ cations with the parent $PbX_2$ structures leads to a rearrangement of the lattice into the observed columnar structure. Groups of six $Et_2NH_2^+$ cations are hydrogen bonded to these columns, girdling them at their narrowest points. These hydrogen bonds contribute to the formation of the zigzag nature of the columnar inorganic framework. The resultant structures are recombinate analogues (polytypes) of the $(Pb_3X_9)_n^{3n-}$ stacks that would be obtained by the dimensional reduction process of the parent layer $PbX_2$ structure into simple edge-shared ribbons of $PbX_6$ octahedra. These structures can be described in terms of the stacking of planar bibridged $Pb_3X_8^{2-}$ units decorated with a single halide ion at a terminal lead ion site. In a similar fashion, ($\beta$-alaH)$_2Sn_2I_6$ contains corrugated $(Sn_2I_6)_n^{2n-}$ columns ($\beta$-ala = $\beta$-alanine), with the cations sitting in the clefts of the columns.

## Introduction

One of the crystal engineering strategies for the design of low-dimensional inorganic materials involves the dimensional reduction of higher dimensional parent structures. Tulsky and Long have applied this concept to describe the types of low-dimensional systems that can be obtained from $MX_n$ structures via reaction with anionic $AX_m$ reagents.[1] However, this strategy is not restricted to these basic systems. For example, from the parent $AMX_3$ perovskite system,[2] this concept can be used to rationalize the synthesis of the layer structures found in the high-$T_c$ copper oxide based superconductors.[3] This concept can be extended to hybrid organic/inorganic materials when $A^{m+}$ is an organic cation. Here again, the dimensional reduction of the $AMX_3$ perovskite structure, where $X^-$ is a halide ion, has yielded many interesting layered $(RNH_3)_2MX_4$ magnetic and semiconducting systems.[4] The resultant two-dimensional framework of corner-shared $MX_6$ octahedra are stabilized by hydrogen bonding between the $-NH_3^+$ moieties of the organoammonium ions and the nonbridging halide ions of the inorganic sheets. This produces a bilayer type structure in which the central inorganic framework is sheathed by the organic R groups.[5] In general, unfortunately, the multiple challenges of diversity of hydrogen-bonding capabilities, ligand-bridging capabilities, and organic steric effects make the prediction of such dimensional reduction schemes uncertain.

The layered hexagonal $MX_2$ structures, consisting of layers of edge-shared octahedra, can also be utilized as a parent template for the design of novel low-dimensional systems.[6] Tulsky and Long have also documented the possible subclasses that are observed from reaction with inorganic AX species.[1] These include perforated layers in which $M^{2+}$

* To whom correspondence should be addressed. E-mail: willett@mail.wsu.edu.

(1) Tulsky, E. G.; Long, J. R. *Chem. Mater.* **2001**, *13*, 1149.
(2) Megaw, H. D. *Nature* **1945**, *155*, 484.
(3) Bednarz, J. G.; Müller, K. A. *Rev. Mod. Phys.* **1988**, *60*, 585.
(4) (a) Mitzi, D. B. *J. Chem. Soc., Dalton Trans.* **2001**, 1. (b) Mitzi D. B.; Chondroudis, K.; Kagan, C. R. *IBM J. Res. Dev.* **2001**, *45*, 29.
(5) Needham, G. F.; Willett, R. D. *J. Chem. Phys.* **1981**, *85*, 3385.
(6) (a) Pauling, L.; Hoard, J. L. *Z. Kristallogr. Kristallgeom. Kristallphys. Kristallchem.* **1930**, *74*, 546. (b) Smirvona, L.; Brager, A.; Zhdanov, H. *Acta Physicochim.* **1941**, *15*, 255.



10.1021/ic020455k CCC: $22.00 
Published on Web 11/22/2002

**Chart 1**

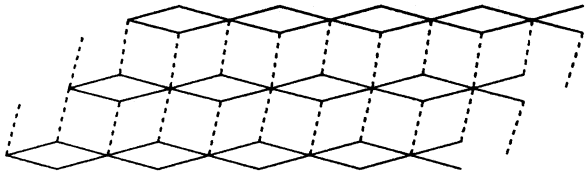

cations are removed from the layers to compensate for the introduction of $A^+$ cations[7] between the layers as well as single and double chains of corner-shared octahedra.[8] We have utilized this concept extensively in our studies of structural and magnetic properties of hybrid organic/inorganic salts of copper(II) halide salts.[9] With the Cu(II) ion, the Jahn−Teller effect leads to a ferrodistortive version of the layered $MX_2$ structure that can be envisioned as stacks of planar bibridged $(CuX_2)_n^n$ linear chains (Chart 1).[10] This resultant structure is particularly susceptible to crystal engineering manipulation. Reaction with organic AX salts can be used to further reduce these chains into smaller planar bibridged $Cu_nX_{2n+2}^{2-}$ oligomers ($n = 1-7$)[11] as well as to perforate the layers.[12]

Recombination[13] of the stacking arrangements of these planar oligomers (via the longer semicoordinate Cu···X bonds induced by the Jahn−Teller effect) leads to a wide variety of polytypes. The structure of two such polytypes for planar $Cu_4X_{10}^{2-}$ anions are shown in Figure 1. The stacking shown in Figure 1a for $(Me_4N)_2Cu_4Cl_{10}$ corresponds to a simple ribbon cut from the parent $CuX_2$ structure.[11a] In contrast, the stacking of the tetramers shown in Figure 1b for $(Me_3NH)_2Cu_4Br_{10}$ represents a polytype in which recombination of the planar oligomers has occurred.[11b] A convenient diagrammatic representation of the stacking patterns observed for these polytypes has been developed, as well as a shorthand notation to specify the repeat pattern in the stacks. Chart 2 illustrates these stacking diagrams for the two polytypes shown in Figure 1. Also given is their designated Geiser notation, $n(t_{||}, t_{\perp})(t'_{||}, t'_{\perp})$.[11c−g] Here $n$ denotes the length of the oligomers, $t_{||}$ denotes the translation parallel to the long axis, and $t_{\perp}$ denotes the relative translation of adjacent anions perpendicular to the long axis, with the $(t_{||}, t_{\perp})$ symbol repeated as often as necessary to describe the repeat pattern in the stack. Stacking patterns with different values of $t_{||}$ and $t_{\perp}$ represent different polytypes. The simple 4(3/2, 1/2) stack in Chart 2a represents a simple dimensional reduction of the layers in the parent $CuX_2$ structures. The more complex 4(3/2, 1/2)(1/2, −1/2) stack in Chart 2b involves further reduction into oligomeric units followed by reconstruction of the semicoordinate interoligomer Cu···X bonds.

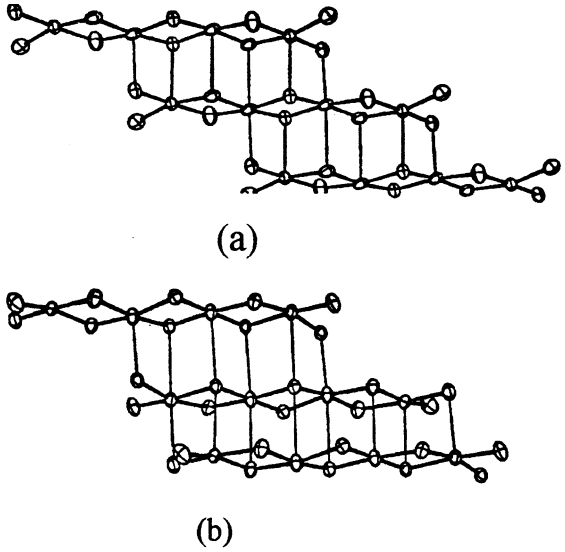


**Figure 1.** Examples of polytypic stacking patterns observed in copper(II) halides: (a) 4(3/2, 1/2) stack in $(Me_4N)_2Cu_4Cl_{10}$; (b) 4(3/2, 1/2)(1/2, −1/2) stack in $(Me_4P)_2Cu_4Br_{10}$.

**Chart 2**

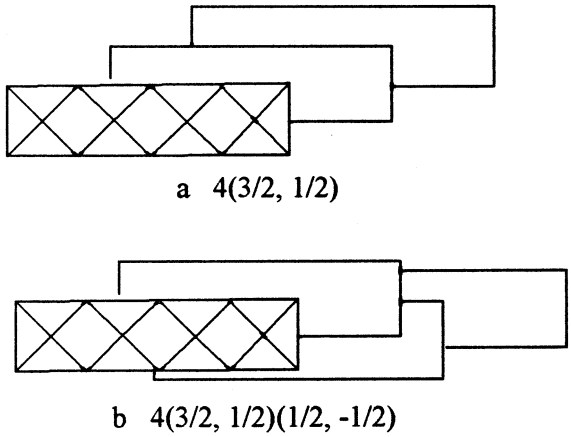


The study of recombination in columnar stacks for hybrid organic/inorganic systems based on the edge-sharing arrangement of octahedra of the $CdX_2$ type has not been as extensive. In the absence of the Jahn−Teller distortion there is no strong directional preference for the dimensional reduction of the parent structure. As documented by Tulsky and Long,[1] the vast majority of the 1-D systems obtained for pure inorganic systems are single or double chains of edge-shared octahedra (Chart 3). For the double chains, planar bibridged $M_2X_6$ units can be identified and the Geiser

(7) (a) Van Loon, C.J.J.; Ijdo, D. J. W. *Acta Crystallogr.* **1975**, *B31*, 770. (b) van Loon, C. J. J.; Verschoor, G. C. *Acta Crystallogr.* **1973**, *B29*, 1224.
(8) (a) Amit, M.; Horowitz, A.; Makovsky, J. *Isr. J. Chem.* **1974**, *12*, 827. (b) Goodyear, J.; Ali, S. A. D.; Steigmann, G. A. *Acta Crystallogr.* **1971**, *B27*, 1672.
(9) (a) Willett, R. D.; Place, H.; Middleton, M. *J. Am. Chem. Soc.* **1988**, *110*, 8639. (b) Willett, R. D. *Acta Crystallogr.* **1998**, *B54*, 503. (c) Halvorson, K.; Patterson, C.; Willett, R. D. *Acta Crystallogr.* **1990**, *B46*, 508. (d) Scott, B.; Willett, R.D. *J. Appl. Phys.* **1987**, *61*, 3289. (e) Geiser, U.; Gaura, R. M.; Willett, R. D.; West, D. X. *Inorg. Chem.* **1986**, *25*, 4203; (f) O'Brien, S.; Gaura, R. M.; Landee, C. P.; Ramakrishna, B. L.; Willett, R. D. *Inorg. Chim. Acta* **1987**, *141*, 83.
(10) Wells, A. F. *J. Chem. Soc.* **1947**, 1670.
(11) (a) Halvorson, K. E.; Grigereit, T.; Willett, R. D. *Inorg. Chem.* **1987**, *26*, 1716. (b) Geiser, U.; Willett, R. D.; Lindbeck, M.; Emerson, K. *Inorg. Chem.* **1986**, *25*, 1173. (c) Willett, R D.; Geiser, U. *Acta Chem. Croat.* **1984**, *57*, 751. (d) Bond, M. R.; Willett, R. D. *Inorg. Chem.* **1984**, *28*, 3267. (e) Willett, R. D.; Bond, M. R.; Pon, G. *Inorg. Chem.* **1990**, *29*, 4160. (f) Willett, R. D. *Acta Crystallogr.* **1993**, *A49*, 613.
(12) Weiss, S.; Willett, R. D. *Acta Crystallogr.* **1993**, *B49*, 283.
(13) The Nomenclature Commission of the International Union of Crystallography in its report on "Nomenclature of Inorganic Structure Types" defines "recombination structures" as those "formed when topologically simple parent structures are periodically divided into blocks, rods or slabs which in turn are recombined into derivative structures by one or more structure building operations".

**Chart 3**

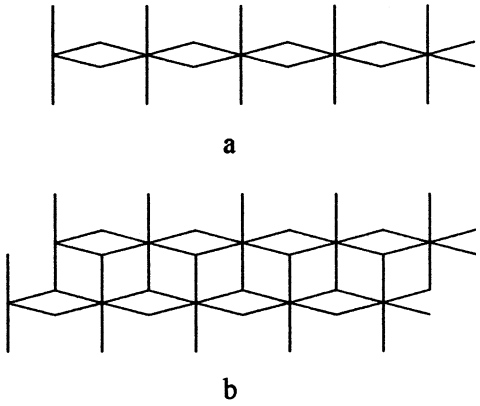


notation can be applied to this type of system, yielding a 2(1/2,1/2) stack designation.[14] Moreover, a search of the Cambridge Database for hybrid organic/organic structures with extended edge-shared octahedral networks revealed only a limited number examples and none involved recombinant structures. However, no examples of polytypes of this structure appear to exist in the simple inorganic systems.

In this paper, three new and novel hybrid organic/inorganic columnar structures are reported. The first of these are for the isostructural $(DEA)_3Pb_3Br_9$ and $(DEA)_3Pb_3I_9.{}^1/_2H_2O$ compounds, where DEA is diethylammonium. For several years, we have had interest in the structural properties of the metal halide salts of the diethylammonium cation. Many of these salts contain $MX_4^{2-}$ anions and exhibit interesting structural phase transitions.[15a−c] A few compounds have previously been found to contain extended inorganic frameworks. The compound $(DEA)_2Cu_4Br_{10}$·EtOH salt contains chains of edge-shared tetrahedra in addition to stacks of $Cu_3Br_8^{2-}$ anions with a 3(1/2, 1/2)(−1/2, −1/2) stacking pattern.[15d] In contrast, the structure of $(DEA)_3Cd_2Br_7$ contains chains of face-shared $CdBr_6$ octahedra plus isolated $CdBr_4^{2-}$ ions.[15e] In addition, we report on the structure of $(\beta\text{-alaH})_2Sn_2I_6$, which also contains a recombinatorial columnar structure. This compound arose as part of our efforts to understand the range of organoammonium cations that can be incorporated in the Sn(II) and Pb(II) halide layer perovskite structures.[16] These represent the first examples of polytypic structures based on dimensional reduction and recombination of the hexagonal $MX_2$ structure type.

## Experimental Section

**Synthesis.** The lead(II) bromide salt was prepared by reacting (DEA)Br and $PbBr_2$ in a 2:1 ratio in a deficiency of $H_2O$ at ∼70 °C in a sealed test tube. The solution was allowed to cool, and at a later date, crystals were removed from the tube. A small colorless crystal (0.3 × 0.3 × 0.1 mm) was selected for the X-ray diffraction study.

The corresponding lead(II) iodide salt was prepared by the reaction of (DEA)Cl and $PbI_2$ in a 1:1 ratio in a concentrated (6 M) HI solution. The resulting solution was slowly evaporated until crystals formed. The crystals were separated from the mother liquor, and a crystal of dimensions 0.14 × 0.07 × 0.03 mm was selected for the diffraction study.

Crystals of $(\beta\text{-alaninium})_2SnI_4$ [$(\beta\text{-alaH})_2SnI_4$] were grown from a slowly cooled 2-butanol/hydriodic acid solution containing 0.323 g ($3.6 \times 10^{-3}$ mol) of $\beta$-alanine and 0.671 g ($1.8 \times 10^{-3}$ mol) of $SnI_2$ (Aldrich, anhydrous beads, 99.999%). These were placed in a test tube under an inert atmosphere, and 10 mL of concentrated (57 wt %) aqueous hydriodic acid was added with a syringe. The components in the tube were thoroughly mixed and then heated to 100 °C. The solution was cooled at 4.4 °C/h to −10 °C, yielding 0.86 g (86% theoretical yield) of yellow/orange, rod-shaped crystals. The crystals were filtered in an inert atmosphere. Chemical analysis of $(\beta\text{-alaH})_2SnI_4$ yielded the following. Calcd: C, 16.99; H, 3.4; N, 3.47. Found: C, 16.67; H, 2.34; N, 3.18.

**X-ray Diffraction.** Data for all three compounds were collected on a Bruker 3-circle platform diffractometer equipped with a SMART 1K CCD detector. The frame data were acquired with the SMART[17] software at 295 K using Mo Kα radiation ($\lambda = 0.710\ 73$ Å). The frames were then processed using the SAINT software[18] to give the *hkl* file corrected for *Lp*/decay. The absorption correction was performed using the SADABS[19] program. The structures were solved by the direct method using the SHELX-90[20] program and refined by least-squares method on $F^2$, SHELXL-93,[21] incorporated in SHELXTL V 5.03.[22] Hydrogen atoms were included in calculated positions. All non-hydrogen atoms were refined anisotropically. The lead(II) bromide and iodide salts were isostructural; however, the room-temperature data set for the iodide salt clearly showed disorder of the ethyl groups on the cations. Hence, a second data set was collected at −70 °C. This also showed disorder of the ethyl groups. Consequently, the cations were thus refined with the C−N and C−C distances loosely constrained. In addition, the difference electron density maps revealed the presence of a partially occupied water molecule site nearly equidistant from I(4), I(7), I(9), and I(11). This was included with an assumed occupancy of 0.5. Data collection and refinement parameters are given in Table 1, while Tables 2−4 give selected bond distances and angles.

## Results

**Lead(II) Halide Salts.** Figure 2 shows the contents of the asymmetric unit of the bromide salt, with the addition of symmetry-related $Br^-$ ions to complete the octahedral coordination sphere of the three $Pb^{2+}$ ions. The iodide salt has an identical lead/halide core. The coordination spheres for both Pb(1) and Pb(3) show significant variations in the Pb−X bond lengths, with those to X(7) and X(11) being

(14) Because of the lack of the presence of a ferrodistortive distortion in these structures, two possible orientations for the planar bibridged $M_2X_6$ units can be identified. Nevertheless, in more complex structures, it is frequently possible to identify an optimal orientation to describe the stacking.

(15) (a) Bloomquist, D. R.; Willett, R. D. *Acta Crystallogr*. **1981**, *B37*, 1353. (b) Bloomquist, D. R.; Pressprich, M. R.; Willett, R. D. *J. Am. Chem. Soc.* **1988**, *110*, 7391. (c) Willett, R. D. *Acta Crystallogr*. **1991**, *C47*, 1083. (d) Fletcher, R.; Hansen, J. J.; Livermore, J.; Willett, R. D. *Inorg. Chem.* **1982**, *21*, 330. (e) Willett, R. D.; Twamley, B. *Acta Crystallogr*. **2001**, *E57*, m573.

(16) For a general review, see: Mitzi, D. B. *Prog. Inorg. Chem.* **1999**, *48*, 1.

(17) *SMART V4.045 Software for the CCD Detection system*; Bruker AXS Inc.: Madison, WI, 1996.

(18) *SAINT V 4.035 Software for the CCD Detector System*; Bruker AXS, Inc.: Madison, WI, 1996.

(19) *SADABS Program for Absorption Correction for Area Detectors*; Bruker AXS Inc.: Madison, WI, 1996.

(20) Sheldrick, G. M. *SHELXS-90 Program for the Solution of Crystal Structure*; University of Göttingen: Göttingen, Germany, 1986.

(21) Sheldrick, G. M. *SHELXL-97 Program for the Refinement of Crystal Structures*; University of Göttingen: Göttingen, Germany, 1997.

(22) *SHELXTL 5.10 (PC-Version) Program Library for Structure Solution and Molecular Graphics*; Bruker AXS Inc.: Madison, WI, 1997.

**Table 1.** Crystal Data and Structure Refinement Parameters

| empirical formula | $C_{12}H_{36}N_3Pb_3Br_9$ | $C_{12}H_{37}N_3O_{.5}Pb_3I_9$ | $C_6H_{16}N_2O_4Sn_2I_6$ |
|---|---|---|---|
| fw | 1563.20 | 1986.11 | 1178.99 |
| $T$ (K) | 293(2) | 183(2) | 81(2) |
| space group | $P2_1/c$ | $P2_1/c$ | $P2_1/c$ |
| $a$ (Å) | 10.753(6) | 11.281(7) | 20.604(3) |
| $b$ (Å) | 23.976(11) | 24.917(15) | 13.146(2) |
| $c$ (Å) | 14.239(6) | 14.371(8) | 8.482(1) |
| $\beta$ (deg) | 111.50(5) | 110.92(1) | 95.75(3) |
| $V$ (Å$^3$) | 3416(3) | 3774(4) | 2286.0(5) |
| Z | 4 | 4 | 4 |
| $\lambda$ (Å) | 0.71073 | 0.71073 | 0.71073 |
| $D_{calc}$ (Mg/m$^3$) | 3.040 | 3.496 | 3.426 |
| $\mu$ (mm$^{-1}$) | 25.284 | 20.722 | 10.297 |
| $R_1$[a] | 0.0458 | 0.0354 | 0.0334 |
| $wR_2$[b] | 0.1085 | 0.0622 | 0.0730 |

[a] $R_1 = \Sigma||F_o| - |F_c||/\Sigma|F_o|^2$. [b] $wR_2 = \{\Sigma[w(F_o^2 - F_c^2)^2/\Sigma[w(F_c^2)^2]\}^{1/2}$.

**Table 2.** Bond Distances (Å) and Angles (deg) for $(DEA)_3Pb_3Br_9$[a]

Distances

| | | | |
|---|---|---|---|
| Pb(1)−Br(9) | 2.807(2) | Pb(2)−Br(7)#2 | 3.038(2) |
| Pb(1)−Br(6) | 2.912(2) | Pb(2)−Br(7) | 3.090(2) |
| Pb(1)−Br(10) | 3.020(2) | Pb(2)−Br(11) | 3.178(2) |
| Pb(1)−Br(5) | 3.085(2) | Pb(3)−Br(8) | 2.787(2) |
| Pb(1)−Br(11)#1 | 3.178(2) | Pb(3)−Br(12) | 2.822(2) |
| Pb(1)−Br(11) | 3.229(2) | Pb(3)−Br(6)#2 | 3.049(2) |
| Pb(2)−Br(4) | 2.877() | Pb(3)−Br(4) | 3.054(2) |
| Pb(2)−Br(10)#1 | 2.958(2) | Pb(3)−Br(7)#2 | 3.272(2) |
| Pb(2)−Br(5) | 3.033(2) | Pb(3)−Br(11)#2 | 3.302 |

Angles

| | | | |
|---|---|---|---|
| Br(9)−Pb(1)−Br(6) | 92.70(7) | Br(10)#1−Pb(2)−Br(7) | 174.31(4) |
| Br(9)−Pb(1)−Br(10) | 95.75(6) | Br(5)−Pb(2)−Br(7) | 90.03(7) |
| Br(6)−Pb(1)−Br(10) | 93.15(6) | Br(7)#2−Pb(2)−Br(7) | 83.78(7) |
| Br(9)−Pb(1)−Br(5) | 91.71(6) | Br(4)−Pb(2)−Br(11) | 176.16(5) |
| Br(6)−Pb(1)−Br(5) | 91.65(6) | Br(10)#1−Pb(2)−Br(11) | 86.15(5) |
| Br(10)−Pb(1)−Br(5) | 170.93(5) | Br(5)−Pb(2)−Br(11) | 88.14(5) |
| Br(9)−Pb(1)−Br(11)#1 | 93.51(6) | Br(7)#2−Pb(2)−Br(11) | 87.05(5) |
| Br(6)−Pb(1)−Br(11)#1 | 173.69(4) | Br(7)−Pb(2)−Br(11) | 88.61(5) |
| Br(10)−Pb(1)−Br(11)#1 | 85.10(5) | Br(8)−Pb(3)−Br(12) | 93.90(6) |
| Br(5)−Pb(1)−Br(11)#1 | 89.31(5) | Br(8)−Pb(3)−Br(6)#2 | 88.84(7) |
| Br(9)−Pb(1)−Br(11) | 176.39(5) | Br(12)−Pb(3)−Br(6)#2 | 92.68(7) |
| Br(6)−Pb(1)−Br(11) | 90.39(6) | Br(8)−Pb(3)−Br(4) | 93.33(7) |
| Br(10)−Pb(1)−Br(11) | 85.95(6) | Br(12)−Pb(3)−Br(4) | 93.83(7) |
| Br(5)−Pb(1)−Br(11) | 86.32(5) | Br(6)#2−Pb(3)−Br(4) | 172.97(5) |
| Br(11)#1−Pb(1)−Br(11) | 83.45(6) | Pb(2)−Br(4)−Pb(3) | 97.58(6) |
| Br(4)−Pb(2)−Br(10)#1 | 91.77(6) | Pb(2)−Br(5)−Pb(1) | 95.54(5) |
| Br(4)−Pb(2)−Br(5) | 95.16(6) | Pb(1)−Br(6)−Pb(3)#2 | 96.84(7) |
| Br(10)#1−Pb(2)−Br(5) | 92.00(7) | Pb(2)#2−Br(7)−Pb(2) | 96.22(7) |
| Br(4)−Pb(2)−Br(7)#2 | 89.87(6) | Pb(2)#1−Br(10)−Pb(1) | 98.04(6) |
| Br(10)#1−Pb(2)−Br(7)#2 | 93.74(7) | Pb(2)−Br(11)−Pb(1)#1 | 90.47(5) |
| Br(5)−Pb(2)−Br(7)#2 | 172.25(5) | Pb(2)−Br(11)−Pb(1) | 89.99(5) |
| Br(4)−Pb(2)−Br(7) | 93.33(6) | Pb(1)#1−Br(11)−Pb(1) | 96.55(6) |

[a] Symmetry transformations used to generate equivalent atoms: #1, $-x$, $-y$, $-z + 2$; #2, $-x + 1$, $-y$, $-z + 2$.

the longest. This is probably due to some degree of localization of the lone pairs on the Pb(II) ions into that region of space. The central feature of this core is the existence of groups of three edge-shared octahedra that defines a linear bibridged $(Pb_3X_8)^{2-}$ unit that can be used to describe the construction of the columnar structure in these two compounds. The framework of the two isostructural compounds consist of corrugated columns of $(Pb_3X_9)_n^{3-}$ stacks that run parallel to the $a$ axis. This is illustrated in Figure 3 for $X = I^-$. The stacks are built up of edge-shared $PbX_6$ octahedra linked together in a kinked zigzag fashion. The complex structure of the stacks is intimately associated with the role played by the hydrogen-bonding interactions between the $DEA^+$ cations and the halide ions in the stacks.

**Table 3.** Bond Distances (Å) and Angles (deg) for $(DEA)_3Pb3I_9 \cdot {}^1/_2H_2O$[a]

Distances

| | | | |
|---|---|---|---|
| Pb(1)−I(9) | 3.033(1) | Pb(2)−I(5) | 3.226(2) |
| Pb(1)−I(6) | 3.127(2) | Pb(2)−I(7) | 3.291(2) |
| Pb(1)−I(10) | 3.229(2) | Pb(2)−I(11) | 3.391(2) |
| Pb(1)−I(5) | 3.238(2) | Pb(3)−I(8) | 3.024(2) |
| Pb(1)−I(11)#1 | 3.337(2) | Pb(3)−I(12) | 3.027(2) |
| Pb(1)−I(11) | 3.372(2) | Pb(3)−I(6)#2 | 3.239(2) |
| Pb(2)−I(4) | 3.087(2) | Pb(3)−I(4) | 3.269(2) |
| Pb(2)−I(10)#1 | 3.165(2) | Pb(3)−I(7)#2 | 3.463(2) |
| Pb(2)−I(7)#2 | 3.207(2) | Pb(3)−I(11)#2 | 3.462(2) |

Angles

| | | | |
|---|---|---|---|
| I(9)−Pb(1)−I(6) | 92.06(5) | I(10)#1−Pb(2)−I(7) | 174.69(3) |
| I(9)−Pb(1)−I(10) | 94.34(4) | I(7)#2−Pb(2)−I(7) | 87.91(5) |
| I(6)−Pb(1)−I(10) | 92.14(4) | I(5)−Pb(2)−I(7) | 86.36(5) |
| I(9)−Pb(1)−I(5) | 89.26(4) | I(4)−Pb(2)−I(11) | 178.57(3) |
| I(6)−Pb(1)−I(5) | 89.17(4) | I(10)#1−Pb(2)−I(11) | 87.95(4) |
| I(10)−Pb(1)−I(5) | 176.12(3) | I(7)#2−Pb(2)−I(11) | 87.23(3) |
| I(9)−Pb(1)−I(11)#1 | 87.96(5) | I(5)−Pb(2)−I(11) | 88.48(3) |
| I(6)−Pb(1)−I(11)#1 | 179.98(4) | I(7)−Pb(2)−I(11) | 86.89(4) |
| I(10)−Pb(1)−I(11)#1 | 87.86(4) | I(8)−Pb(3)−I(12) | 92.82(4) |
| I(5)−Pb(1)−I(11)#1 | 90.84(4) | I(8)−Pb(3)−I(6)#2 | 93.46(5) |
| I(9)−Pb(1)−I(11) | 175.88(2) | I(12)−Pb(3)−I(6)#2 | 89.94(4) |
| I(6)−Pb(1)−I(11) | 91.45(5) | I(8)−Pb(3)−I(4) | 91.03(5) |
| I(10)−Pb(1)−I(11) | 87.69(3) | I(12)−Pb(3)−I(4) | 98.37(4) |
| I(5)−Pb(1)−I(11) | 88.62(3) | I(6)#2−Pb(3)−I(4) | 170.35(3) |
| I(11)#1−Pb(1)−I(11) | 88.54(5) | Pb(2)−I(4)−Pb(3) | 95.16(3) |
| I(4)−Pb(2)−I(10)#1 | 91.75(4) | Pb(2)−I(5)−Pb(1) | 94.08(3) |
| I(4)−Pb(2)−I(7)#2 | 91.39(4) | Pb(1)−I(6)−Pb(3)#2 | 94.28(5) |
| I(10)#1−Pb(2)−I(7)#2 | 93.07(5) | Pb(2)#2−I(7)−Pb(2) | 92.09(5) |
| I(4)−Pb(2)−I(5) | 92.93(3) | Pb(2)#1−I(10)−Pb(1) | 95.11(4) |
| I(10)#1−Pb(2)−I(5) | 92.28(5) | Pb(1)#1−I(11)−Pb(1) | 91.46(5) |
| I(7)#2−Pb(2)−I(5) | 173.02(3) | Pb(1)#1−I(11)−Pb(2) | 89.07(4) |
| I(4)−Pb(2)−I(7) | 93.44(4) | Pb(1)−I(11)−Pb(2) | 88.75(3) |

[a] Symmetry transformations used to generate equivalent atoms: #1, $-x$, $-y$, $-z + 2$; #2, $-x + 1$, $-y$, $-z + 2$.

**Table 4.** Bond Distances (Å) and Angles (deg) for $(\beta\text{-alaH})_2Sn_2Cl_6$[a]

Distances

| | | | |
|---|---|---|---|
| Sn(1)−I(1) | 3.202(1) | Sn(2)−I(3) | 3.645(1) |
| Sn(1)−I(2) | 2.923(1) | Sn(2)−I(3)#1 | 3.285(1) |
| Sn(1)−I(1)#1 | 3.114(1) | Sn(2)−I(4) | 3.046(1) |
| Sn(1)−I(3) | 3.615(1) | Sn(2)−I(5) | 3.286(1) |
| Sn(1)−I(3)#1 | 3.239(1) | Sn(2)−I(5)#2 | 3.063(1) |
| Sn(1)−I(4) | 3.128(1) | Sn(2)−I(6) | 2.917(1) |

Angles

| | | | |
|---|---|---|---|
| I(2)−Sn(1)−I(1)#1 | 91.18(2) | I(4)−Sn(1)−I(3) | 82.44(2) |
| I(2)−Sn(1)−I(4) | 85.28(2) | I(1)−Sn(1)−I(3) | 103.53(2) |
| I(1)#1−Sn(1)−I(4) | 100.30(3) | I(6)−Sn(2)−I(4) | 86.79(2) |
| I(2)−Sn(1)−I(1) | 89.91(2) | I(6)−Sn(2)−I(5)#2 | 89.12(2) |
| I(1)#1−Sn(1)−I(1) | 86.12(2) | I(4)−Sn(2)−I(5)#2 | 101.32(2) |
| I(4)−Sn(1)−I(1) | 172.03(2) | Sn(1)#2−I(1)−Sn(1) | 100.88(2) |
| I(2)−Sn(1)−I(3) | 162.82(2) | Sn(2)−I(4)−Sn(1) | 107.79(2) |
| I(1)#1−Sn(1)−I(3) | 79.30(1) | | |

[a] Symmetry transformations used to generate equivalent atoms: #1, $x$, $-y + 3/2$, $z - \int$; #2, $x$, $-y + 3/2$, $z + \int$.

As can be seen from Figure 4 for the bromide salt, groups of six $DEA^+$ cations girdle the columnar stacks at their narrowest points. It is this slippage and kinking of the stacks at these points that leads to the recombinatorial structure of these compounds. The main difference in the two structures is the inclusion of a lattice water molecule (at partial occupancy) in the iodide structure, as shown in Figure 3. This lattice water of hydration can form hydrogen bonds to any of the four iodide ions in the cleft in the stack produced by the polytypic nature of the stack. The O···I distances range from 3.20 to 3.50 Å.

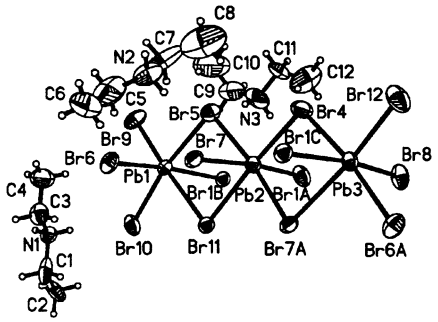


**Figure 2.** Illustration of the asymmetric unit for $(DEA)_3Pb_3Br_9$ (augmented with symmetry-related $Br^-$ ions to complete the Pb coordination spheres).

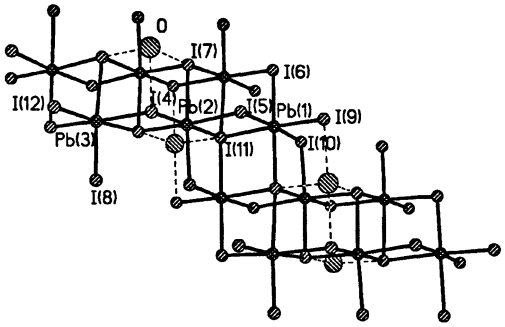


**Figure 3.** Illustration of the $(Pb_3I_9)_n^{3n-}$ columnar structure in $(DEA)_3Pb_3I_9 \cdot {}^1/_2H_2O$, showing the site for the lattice water molecule.

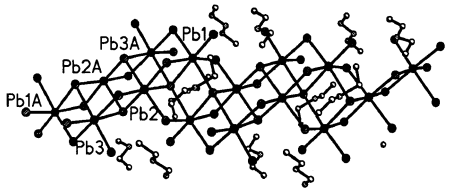


**Figure 4.** Illustration of the $(Pb_3Br_9)_n^{3n-}$ columnar structure in $(DEA)_3Pb_3Br_9$ and the girdling of the columns by sets of six $DEA^+$ cations.

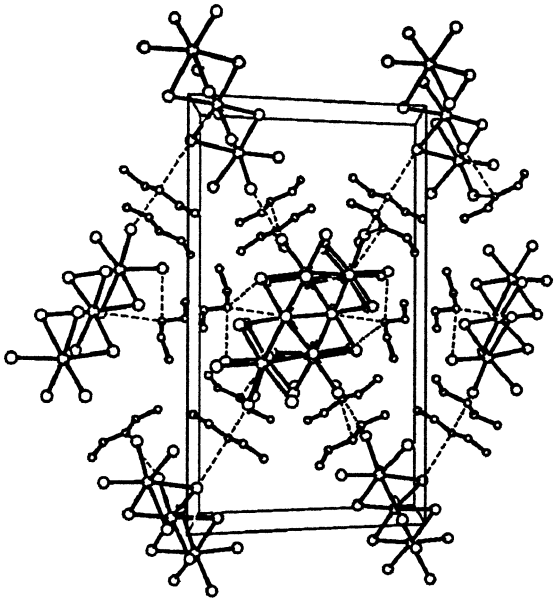

**Figure 5.** Illustration of the packing of the $(Pb_3Br_9)_n^{3n-}$ columns in $(DEA)_3Pb_3Br_9$, showing the hydrogen bonding linking the columns. The view is parallel to the *a* axis, and the *b* axis is vertical.

As illustrated in Figure 5 for X = $Br^-$, these columnar stacks are arranged in a pseudohexagonal fashion, with the stacks running parallel to the *a* axis. Two of the three independent $DEA^+$ cations form linking X···H−N−H···X hydrogen bonding interactions in the [110] directions to provide three-dimensional stability to the lattice. These interactions lead to short X···X contacts between 8 and 9 in adjacent stacks. For the bromide salt, these contact distances are 3.794(3) Å, while the contact distances are 4.002(2) Å in the iodide salt. The third $DEA^+$ cation forms only intrastack hydrogen bonds. The inclusion of the lattice water in the iodide salt does not dramatically affect the N−H···X hydrogen bonding scheme that was observed for the bromide salt. However, it would appear to be associated with the observed reorientation and disorder of the ethyl groups in the $DEA^+$ cations.

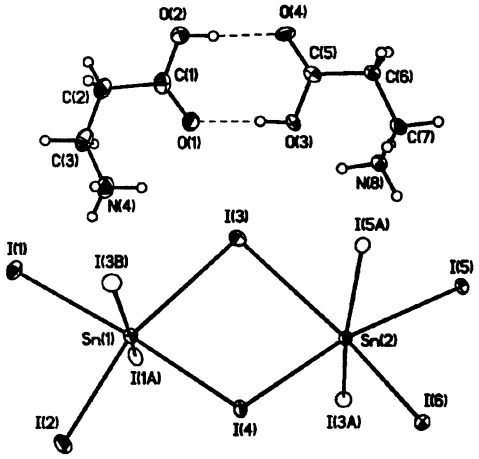


**Figure 6.** Illustration of the asymmetric unit in $(\beta\text{-alaH})_2Sn_2Cl_6$, augmented by additional iodide ions to complete the Sn octahedra.

**Chart 4**

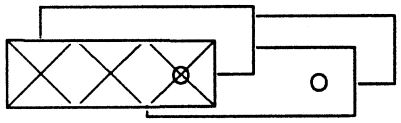

3(1/2, 1/2)(3/2, -1/2)[X]

The columnar structure illustrated in Figure 3 may be viewed as being built up of stacks of the planar $Pb_3X_8^{2-}$ moieties, with each moiety augmented by a $X^-$ ion to complete the octahedral coordination geometry of the terminal Pb ion (Pb(3)) in the moiety. The columns can then be represented by the pattern diagrammed in Chart 4. An extended Geiser notation can be developed to designate this pattern, 3(1/2, 1/2)(3/2, 1/2)[X], where the quantity in the brackets specifies the ligand(s) that decorate the planar moiety to complete the octahedral coordination of the metal ion. In the diagrammatic representation in Chart 4, the "o" indicates the position of the additional ligand that decorates the planar moiety.

**$(\beta$-alaH)$_2Sn_2Cl_6$ Structure.** The asymmetric unit of this structure, augmented to complete the very distorted octahedral coordination of the Sn(II) ions, is shown in Figure 6. The bond distances from both Sn atoms to I(3) are substantially longer than the others (3.645, 3.615 Å). Concomitantly, the distances to the iodide ions trans to I(3) are the shortest. This is presumably due to the localization

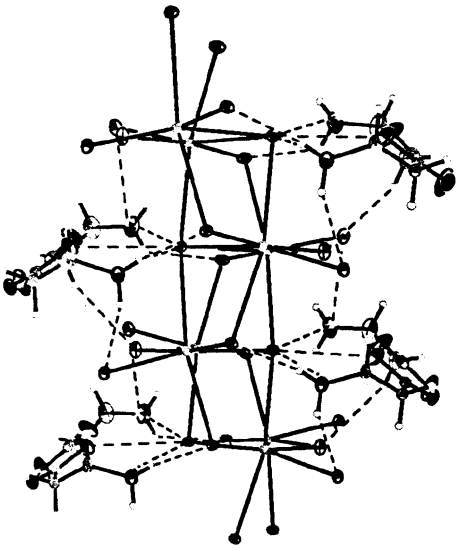

**Figure 7.** Illustration of the $(Sn_2I_6)_2^{2n-}$ columnar stack in$(\beta\text{-alaH})_2Sn_2Cl_6$ illustrating the hydrogen bonding of the $(\beta\text{-alaH})_2^{2+}$ dimers in the clefts of the stacks.

**Chart 5**

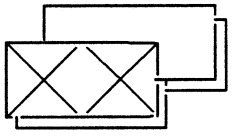

2(1/2, 1/2)(-1/2, -1/2)

of the lone pair of electrons on the Sn(II) ions in the region of the Sn−I(3) bonds. This distortion is significantly larger than in the Pb(II) salts, in accord with the smaller radius of the Sn(II) ion. The $\beta$-alaH$^+$ cations form hydrogen-bonded pairs (O(3)−H(3C)···O(1) = 2.629(7) and O(2)−H(2C)−O(4) = 2.646(7) Å).

The tin/iodide species aggregate into a columnar structure that run parallel to the *c* axis, as seen in Figure 7. In addition, the $-NH_3^+$ moieties of the $\beta$-alaH$^+$ cations hydrogen bond to the $I^-$ ions in a bidendate fashion, as seen in Figure 7. The tin/iodide framework takes on a washboard structure to accommodate this mode of hydrogen bonding. Sitting in the clefts in this framework, the $-NH_3^+$ species hydrogen bond to iodide ions in three $Sn_2I_6$ layers. The stacking diagram for this stack, denoted by the augmented Geiser symbol of 2(1/2, 1/2)(−1/2, −1/2), is shown in Chart 5. This arrangement again corresponds to a recombinatorial structure of the dimer chain illustrated in Chart 3b. The $-CO_2H\cdots HO_2C-$ portions of the stacks shown in Figure 7 interdigitate to form layers lying parallel to the (100) planes, as shown in Figure 8, with weak N−H···I hydrogen bonds tying the layers together.

## Discussion

Examination of the Cambridge Database[23] for hybrid organic/inorganic salts with extended edge-shared octahedra

(23) Cambridge Structural Database, Cambridge Crystallographic Database Centre, 12 Union Road, Cambridge CB2 1EZ, England, 2001.

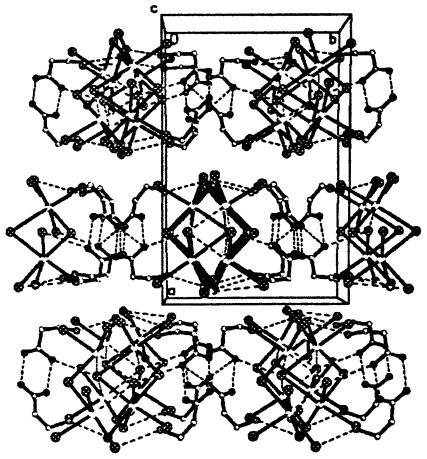


**Figure 8.** Illustration of packing of the $(Sn_2I_6)_2^{2n-}/(\beta\text{-alaH})_2^{2+}$ columns in $(\beta\text{-alaH})_2Sn_2Cl_6$.

structures revealed only a limited number of examples of networks based on dimensional reduction of the parent hexagonal $MX_2$ lattice. No examples of recombinant structures were found. Many of these include coordinated neutral ligands in addition to the halide ions. These can introduce additional steric and/or electronic factors that can lead to variations of the basic structural patterns expected by dimensional reduction arguments. This is amply illustrated in the compounds that contain bibridged chains. Thus, (*N*-methylethylenediammonium)$CdCl_4\cdot 1/2H_2O$ contains linear bibridged chains (Chart 3a) in which the edge sharing is always in a trans configuration.[24] However, in the $PbX_2$-(2-methylpyridine) structures,[25] the coordinated pyridine causes the bridges to assume a cis conformation, while, in $PbI_2(py)_2$, the cis configuration occurs only every sixth metal ion.[26] $(C_3H_7N_2S)CdCl_3$, along with several other compounds, contains double chains of the type shown in Chart 3b.[27] They thus have the simple stacking notation 2(1/2, 1/2) like those noted by Tulsky and Long[1] in the double-chain inorganic salts. A similar situation occurs in $(\varphi_4P)_4[Pb_{15}I_{34}(dmf)_6]$ ($\varphi$ = $C_6H_5$; dmf = dimethylformamide).[28] In this compound, planar bibridged $Pb_3I_8^{2-}$ and $Pb_3I_6(dmf)_2$ units can be identified and the stacking pattern (neglecting the differences in the stoichiometry of the two types of planar moieties) is given by the notation 3(1/2, 1/2) as illustrated in Chart 6a.[29] These *n*(1/2, 1/2) patterns can be viewed as simple ribbons obtained by dimensional reduction of the parent $CdX_2$

(24) (a) Bonamartini-Corradi, A.; Cramarossa, M. R.; Saladini, M. *Inorg. Chim. Acta* **1997**, *257*, 19. (b) Bonamartini-Corradi, A.; Cramarossa, M. R.; Saladini, M.; Battaglia, L. P.; Giusti, J. *Inorg. Chim. Acta* **1995**, *230*, 59.

(25) (a) Engelhardt, L. M.; Patrick, J. M.; Whitaker, C. R.; White, A. H. *Aust. J. Chem.* **1987**, *40*, 2107. (b) Nagapelyan, S. S.; Arakelova, E. R.; Zabrodskii, Yu. R.; Kindyakova, T. V.; Koshkin, V. M.; Mil'ner, A. P.; Slonskay, T. L.; Struckov, Yu. T.; Shklover, V. E. *Zh. Neorg. Khim.* **1990**, *35*, 360.

(26) Miyamae, H.; Tonyama, H.; Abe, T.; Hihara, G.; Nagata, M. *Acta Crystallogr.* **1984**, *C40*, 1559.

(27) Kubiak, M.; Glowiak, T.; Kozlowski, H. *Acta Crystallogr.* **1983**, *C39*, 1637.

(28) Krautscheid, H.; Lekieffre, J. F.; Bessinger, J. *Z. Anorg. Allg. Chem.* **1996**, *622*, 1781.

(29) With labeling of the two moiety units as *a* (for ionic) and *s* (for solvated), the repeat pattern for the moieties in the stack is (*sassa*).

Chart 6

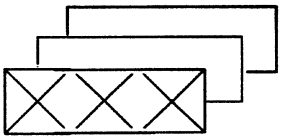

a 3(1/2, 1/2)

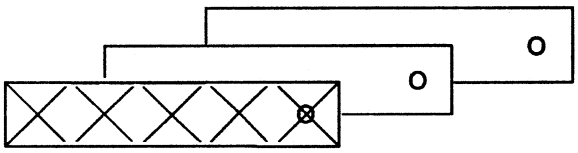


b 5(3/2, 1/2) [X]

structure. A second type of ribbon obtained by the dimensional reduction process has stacking patterns denoted by the notation $n(3/2, 1/2)X_2$. Bonomartini-Corradi et al. reported two structures with this type of pattern. This includes the structure of (*N*-ethylethylenediammonium)$_2Cd_4Cl_{12}\cdot H_2O$ and the structure of $(C_7H_{16}N)_2[Cd_5Cl_{12}(H_2O)_2]\cdot H_2O$.[30] The former contains planar bibridged $Cd_4Cl_{10}^{2-}$ oligomers decorated with pairs of chloride ions, while the latter contains planar bibridged $Cd_5Cl_{12}^{2-}$ oligomers decorated with pairs of water molecules. The latter form stacks shown in Chart 6b. An even more complex ribbon is found in $Cd_3Br_6(H_2O)(DMSO)_2\cdot H_2O$, where a 3(1/2, 1/2)(3/2, 1/2)[X] stacking pattern is observed.[32] Compare this stacking pattern (Chart 7) with that observed in the lead halide salts reported in this paper (Chart 4). All of these stacks may be viewed as ribbons

Chart 7

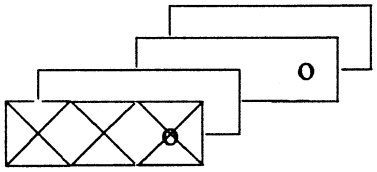


3(1/2,1/2)(3/2,1/2)[X]

obtained via dimensional reduction of the parent layered $MX_2$ structure.

Finally, it should be noted that the compound $(C_5H_{12}ClN_2)Hg_2Cl_5$ contains a perforated $MX_2$ layer in which $Hg_2Cl_2^{2+}$ units are removed from the layer,[30] similar to the $(MeEt_3N)Cu_3Cl_7$ structure where $Cu_2Cl_2^{2+}$ units are excised.[12] This type of perforation was not found by Tulsky and Long[1] in their summary of purely inorganic layered structures of this type.

In summary, this study further demonstrates the potential of using hybrid organic/inorganic systems to produce metal halide structures with novel polymeric structures. This capability has been demonstrated effectively, for example, in the development of semiconducting and conducting Pb(II) and Sn(II) layer perovskite systems.[4] In general, the combination of diverse hydrogen-bonding capabilities and steric effects causes subtle changes in the ways that the metal halide coordination polyhedra can self-assemble in the solid state. Given the unusual results from this study, continued exploration of the structural chemistry of hybrid organic/inorganic metal halide salts is needed to delineate the structural diversity of such systems.

**Supporting Information Available:** Crystal data for all three compounds in CIF format. This material is available free of charge via the Internet at http://pubs.acs.org.

IC020455K

(30) Bonomartini-Corradi, A.; Cramarossa, M. R.; Pellacani, G. C.; Battaglia, L P.; Giusti, J. *Gazz. Chim. Ital.* **1994**, *124*, 481.
(31) Nieuwenhuyzen, M.; Wilkins, C. J. *J. Chem. Soc., Dalton Trans.* **1993**, 2673.
(32) Aharoni, A.; Kapon, M.; Reisner, G. M. *Acta Crystallogr.* **1989**, *C45*, 40.